Carcinogenesis vol.29 no.11 pp.2236–2242, 2008
doi:10.1093/carcin/bgn204
Advance Access publication August 27, 2008

Reduction of brain metastases in plasminogen activator inhibitor-1-deficient mice with transgenic ocular tumors

C.M.Maillard[1,*], C.Bouquet[2], M.M.Petitjean[1], M.Mestdagt[1], E.Frau[2], M.Jost[1], A.M.Masset[1], P.H.Opolon[2], F.Beermann[4], M.M.Abitbol[3], J.M.Foidart[1,5], M.J.Perricaudet[2] and A.C.Noël[1]

[1]Laboratory of Tumor and Development Biology, GIGA-Cancer, Tour de Pathologie (B23), University of Liège, Sart-Tilman, B-4000 Liège, Belgium, [2]CNRS UMR 8121 Univ Paris Sud, Vectorologie et Transfert de Gènes, Institut Gustave Roussy, 39 rue Camille Desmoulins, 94805 Villejuif, France, [3]Centre d'études et de Recherches Thérapeutiques en Ophtalmologie, Faculté de Médecine Necker, 156 rue de Vaugirard, 75015 Paris, France, [4]Swiss Institute for Experimental Cancer Research (ISREC), Faculty of life Sciences, Ecole Polytechnique Fédérable de Lausanne (EPFL), Chemin de Boveresses 155, CH-1066 Epalinges, Switzerland and [5]Department of Gynecology and Obstetrics, CHU, B-4000 Liège, Belgium

[*]To whom correspondence should be addressed. Laboratory of Tumor Biology and Development, Institute of Pathology CHU-B23, University of Liège, Sart-Tilman, B-4000 Liège, Belgium. Tel: +32 4 366 25 69; Fax: +32 4 366 29 36; Email: cmaillard@ulg.ac.be
Correspondence may also be addressed to A.C.Nöel.
Email: agnes.noel@ulg.ac.be

Plasminogen activator inhibitor-1 is known to play a paradoxical positive role in tumor angiogenesis, but its contribution to metastatic spread remains unclear. We studied the impact of plasminogen activator inhibitor *(PAI)-1 deficiency* in a transgenic mouse model of ocular tumors originating from retinal epithelial cells and leading to brain metastasis *(TRP-1/SV40 Tag mice)*. *PAI-1* deficiency did not affect primary tumor growth or vascularization, but was associated with a smaller number of brain metastases. Brain metastases were found to be differentially distributed between the two genotypes. *PAI-1*-deficient mice displayed mostly secondary foci expanding from local optic nerve infiltration, whereas wild-type animals displayed more disseminated nodules in the scissura and meningeal spaces. SuperArray GEarray analyses aimed at detecting molecules potentially compensating for *PAI-1* deficiency demonstrated an increase in fibroblast growth factor-1 (FGF-1) gene expression in primary tumors, which was confirmed by reverse transcription–polymerase chain reaction and western blotting. Our data provide the first evidence of a key role for PAI-1 in a spontaneous model of metastasis and suggest that angiogenic factors, such as FGF-1, may be important for primary tumor growth and may compensate for the absence of PAI-1. They identify PAI-1 and FGF-1 as important targets for combined antitumor strategies.

Introduction

Angiogenesis—the formation of new blood vessels—is an important rate-limiting step during tumor growth and metastatic dissemination. This process requires the co-ordinated regulation of adhesive, proteolytic and migrating events involving different proteolytic systems. Many clinical studies have established a correlation between adverse outcome in patients with multiple cancer types and high levels of serine proteases of the plasminogen activator (PA) system such as the urokinase-type plasminogen activator (uPA) and tissue-type plasminogen activator (tPA) (for review, see refs 1–3). Both uPA and tPA are inhibited by several serine protease inhibitors (Serpins) including plasminogen activator inhibitor (PAI)-1, PAI-2, PAI-3 (protein C inactivator), protease nexin-1 and mammary serine protease inhibitor (Maspin) (1,4). In addition to its inhibitory role during PA-mediated proteolysis, PAI-1 also interacts with vitronectin involved in cell adhesion and migration (5,6), and low-density lipoprotein receptor-related protein implicated in the endocytosis of cell surface molecules (7,8).

As an inhibitor of uPA, PAI-1 was long thought to be an inhibitor of tumorigenesis and angiogenesis. A high level of PAI-1 protein in extracts of human primary malignant tumors is one of the most informative biochemical markers of a poor prognosis in several human cancer types (2,3,9). A dose-dependent effect of PAI-1 on pathological angiogenesis has been observed both *in vitro* (10) and *in vivo* (11–14). Tumor growth and angiogenesis are impaired in mice with a *PAI-1* gene deletion (15–17) or following the induction of PAI-1 expression at supraphysiological levels by adenoviral gene transfer or tumor cell transfection, the administration of recombinant PAI-1 protein and in transgenic mice overexpressing *PAI-1* (12,14,18–20).

The impact of PAI-1 on metastatic dissemination is less clear. An increase in pulmonary metastasis has often been observed in response to PAI-1 administration (21,22). However, other studies have reported no difference in metastatic dissemination with PAI-1 level (23,24). It should be pointed out that these data obtained after induction of experimental tumors by massive tumor cell injection may not be representative of events in the pathogenesis of real cancers. Many of the models used to study metastasis bypass the early events of tumor progression toward a metastatic stage. Genetically engineered mouse models that spontaneously develop cancer in a target organ may thus provide a powerful tool for more accurately mimicking the natural history of cancer. A single study has evaluated the impact of *PAI-1* deficiency in a transgenic mouse model of cancer (24). Primary breast tumor development and lung metastasis were similar in *MMTV-PymT* mice with and without PAI-1 expression (24). It remains unclear whether possible compensatory or redundant mechanisms can mediate tumor angiogenesis and metastatic dissemination in the absence of PAI-1. The aim of this paper is to evaluate the role of PAI-1 on tumor metastasis and to search for putative factors that could substitute for PAI-1 in genetically induced tumors. We backcrossed *PAI-1*-deficient mice with *TRP-1/SV40 Tag* transgenic mice, which spontaneously develop ocular tumors derived from retinal pigmented epithelium (RPE), leading to brain metastasis (25). While *PAI-1* deficiency has no effect on primary ocular tumor growth, it reduces the number of metastatic foci and affects their distribution in the brain. The present paper reports for the first time that PAI-1 contributes to the early steps of metastatic dissemination in a transgenic mouse tumor model recapitulating all the steps of metastasis. Attempts to identify molecules potentially compensating for *PAI-1* deficiency, we have demonstrated an increase in levels of messenger RNA (mRNA) and protein for fibroblast growth factor-1 (FGF-1) in primary tumors.

Abbreviations: GAPDH, glyceraldehyde 3-phosphate dehydrogenase; FGF-1, fibroblast growth factor-1; KO, knockout; Maspin, mammary serine protease inhibitor; MMP, matrix metalloproteinase; mRNA, messenger RNA; PA, plasminogen activator; PAI, plasminogen activator inhibitor; RPE, retinal pigmented epithelium; RT–PCR, reverse transcription–polymerase chain reaction; Serpin, serine protease inhibitors; TIMP, tissue inhibitor of metalloprotease; tPA, tissue-type plasminogen activator; TRP-1, tyrosine-related protein 1; uPA, urokinase-type plasminogen activator; VEGF, vascular endothelial growth factor; WT, wild-type.

Materials and methods

Genetically modified mice

TRP-1/SV40 Tag transgenic mice were generated by insertion into Y chromosome of a 1.4 kb fragment of tyrosine-related protein 1 (TRP-1) promoter fused to SV40 Tag transforming sequence (25). Female *PAI-1*-deficient mice *(PAI-1$^{-/-}$)* (15) in C57BL/6J background were mated with male *TRP-1/SV40 Tag* transgenic mice. These *TRP-1/SV40 Tag PAI-1$^{+/-}$* males were backcrossed to C57BL/6J for six generations. *TRP-1/SV40 Tag PAI-1$^{-/-}$* mice were obtained by breeding these males to *PAI-1$^{-/-}$* females or *PAI-1$^{+/+}$* [wild-type (WT)] female littermates. Mouse experimentation was done in accordance to the guidelines of the University of Liège regarding the care and use of laboratory animals.

Tissue sample collection and brain metastasis analysis

For histological analysis, animals were killed 64 days after birth. The entire head of each animal was fixed in 4% formalin. After overnight decalcification (Sakura Finetek, Zoeterwoude, The Netherlands), tissue samples were rinsed in water for 1 h and incubated in 4% formalin for 1 h. Five frontal fragments of the head were cut to isolate several brain areas covering the entire organ. Paraffin sections cut from each head fragment (five per animal) were stained with hematoxylin and eosin. Total number of metastases per mouse was determined as the number of metastatic foci on five sections for each animal ($n = 22$ for *PAI-1*$^{-/-}$ and $n = 19$ for WT mice). Incidence of metastasis was calculated as the percentage of mice with one or more metastatic nodules in the brain. Metastasis severity was scored as follows: minimal (score 0 = no metastatic nodule), medium (score 1 = <4 metastatic nodules) or extensive involvement (score 2 = 5–7 metastatic nodules).

Isolation of tumor cells and chemotactic assay

To isolate RPE tumor cells, eyes of *TRP-1/SV40* mice proficient ($n = 5$) or deficient ($n = 5$) in *PAI-1* were dissected and cut in small pieces (~0.5 mm^3). Tumor explants transferred to culture plates were grown in Dulbecco's modified Eagle's medium supplemented with 10% fetal calf serum. After 2 weeks of culture, cells that had spread from the explants were trypsinized and kept in culture for at least 6 weeks. Cells were then passaged >10 times before phenotyping. The absence of contaminating cells was checked by immunocytochemistry using an antibody directed against SV40 large T antigen (Sigma, St Louis, MO) (25). Migratory properties of RPE cells were assessed by using the Boyden chamber assay. RPE cells (50 000) were suspended in serum-free medium (300 µl) supplemented with 0.1% bovine serum albumin (Sigma, St Louis, MO) and placed in the upper compartment of a 24-well transwell (8 µm pore size, 6.5 mm diameter, Costar, NY) coated with gelatine (5 µg per filter). The lower compartment was filled with 600 µl of medium containing 5% fetal calf serum and 1% bovine serum albumin as chemoattractant. After 5 h of incubation, the filters were rinsed once in phosphate-buffered saline, fixed in −20°C methanol for 30 min and stained with 0.1% crystal violet (Sigma) for 20 min. Cells on the upper surface of the filters were wiped away with a cotton swab. Cells on the lower surface were detached by setting the filter in 50 µl 10% acetic acid. Migration was quantified by measuring the absorbance of crystal violet at 560 nm.

Gene array

Total RNA was extracted from the eyes of 10 *TRP-1/PAI-1*$^{-/-}$ and 9 control *TRP-1/PAI-1*$^{+/+}$ mice (2 months old), using High Pure RNA isolation kit (Roche Diagnostics, Mannheim, Germany). Relative mRNA expression levels were determined for genes involved in tumor progression and cancer metastasis, using the GEarray (SuperArray, Frederick, MD), according to the manufacturer's protocol. Array images were digitized by densitometric scanning on a Fluor-S MultiImager (Bio-Rad Laboratories, Hercules, CA) and analyzed by using GEarray Expression Analysis Suite software (SuperArray). Values were normalized with respect to the signal for a housekeeping gene *glyceraldehyde-3-phosphate dehydrogenase* (*GAPDH).* Genes were considered to be differentially expressed if the ratio between control and *PAI-1*$^{-/-}$ mice was >1.5.

Reverse transcription–polymerase chain reaction analysis

Reverse transcription–polymerase chain reaction (RT–PCR) amplification was carried out with the GeneAmp Thermostable rTth reverse transcriptase RNA PCR kit (Perkin Elmer Life Sciences, Boston, MA) with specific pairs of primers (Table I). RT–PCR products were resolved by electrophoresis in 10% polyacrylamide gels and analyzed with a Fluor-S MultiImager after staining with Gelstar dye (FMC BioProducts, Heidelberg, Germany). RT–PCR products were quantified by normalization with respect to 28S ribosomal ribonucleic acid.

Western blotting

Entire eyes collected on day 64 were placed in lysis tubes (MagNA Lyser Green Beads, Roche Diagnostics) containing 300 µl of lysis buffer (50 mM Tris–HCl, pH 7.5; 110 mM NaCl; 10 mM ethylenediaminetetraacetic acid; 5 mM iodoacetamide and 0.1% NP40). Protein extracts were collected by centrifugation at 12 000 r.p.m., at 4°C for 30 min. Protein concentration was determined with DC Protein Assay Kit (Bio-Rad Laboratories). Samples (30 µg of protein) were resolved by sodium dodecyl sulfate–polyacrylamide gel electrophoresis in 15% polyacrylamide gels under reducing conditions and proteins were transferred to polyvinylidene difluoride membranes (NEN, Boston, MA). Membranes were incubated for 2 h in blocking Tris-buffered saline buffer (25 mM Tris–HCl, pH 7.6; 150 mM NaCl and 0.1% Tween 20) supplemented with 5% non-fat milk powder. They were then incubated overnight with a polyclonal goat antibody directed against human FGF-1 (R&D systems, Minneapolis, MN). Membranes were washed and incubated for 1 h with secondary horseradish peroxidase-conjugated rabbit anti-goat antibody (DAKO, Glostrup, Denmark). Signals were detected with an enhanced chemiluminescence kit (Perkin Elmer Life Sciences) according to the manufacturer's instructions. GAPDH detection was carried out (using a rabbit antibody, R&D systems) on the same membranes, as a control.

Statistical analysis

Statistical differences between experimental groups were assessed with Mann–Whitney test. Chi-squared analysis was used to compare metastasis incidence between groups. Log-rank tests were used to compare survival curves. Prism 4.0 software (GraphPad, San Diego, CA) was used and *P*-values <0.05 were considered significant.

Results

PAI-1 gene deficiency does not prevent the development of primary ocular tumors

Primary ocular tumor development was monitored at day 64 after birth in a cohort of *TRP-1 PAI-1*$^{-/-}$ ($n = 22$) and *TRP-1 PAI-1*$^{+/+}$ (WT, $n = 19$) mice (Figure 1A and B). In mice of both genotypes, the entire eyeball and optic nerves were completely filled by cuboidal neoplastic cells arranged in a tubular fashion, similar to that observed

Table I. Sequences of primers used for RT–PCR studies

	Forward primer (5′ → 3′)	Reverse primer (5′ → 3′)	Cycles (*n*)
MMP-2	5′-AGATCTTCTTCTTCAAGGACCGGTT-3′	5′-GGCTGGTCAGTGGCTTGGGGTA-3′	27
MMP-9	5′-GCGGAGATTGGGAACCAGCTGTA-3′	5′-GACGCGCCTGTGTACACCCACA-3′	35
MMP-13	5′-ATGATCTTTAAAGACAGATTCTTCTGG-3′	5′-TGGGATAACCTTCCAGAATGTCATAA-3′	33
MMP-14	5′-GGATACCCAATGCCCATTGGCCA-3′	5′-CCATTGGGCATCCAGAAGAGAGC-3′	27
TIMP-1	5′-CATCCTGTTGTTGCTGTGGCTGAT-3′	5′-GTCATCTTGATCTCATAACGCTGG-3′	30
TIMP-2	5′-CTCGCTGGACGTTGGAGGAAAGAA-3′	5′-AGCCCATCTGGTACCTGTGGTTCA-3′	25
TIMP-3	5′-CTTCTGCAACTCCGACATCGTGAT-3′	5′-CAGCAGGTACTGGTACTTGTTGAC-3′	27
RECK	5′-GGCCCTTGCCAGCCTTTCTGCAGA-3′	5′-ACAGCAAGCCCCTGGTGGGATGA-3′	33
uPA	5′-ACTACTACGGCTCTGAAGTCACCA-3′	5′-GAAGTGTGAGACTCTCGTGTAGAC-3′	30
tPA	5′-CTACAGAGCGACCTGCAGAGAT-3′	5′-AATACAGGGCCTGCTGACACGT-3′	27
uPAR	5′-ACTACCGTGCTTCGGGAATG-3′	5′-ACGGTCTCTGTCAGGCTGATG-3′	30
PAI-1	5′-AGGGCTTCATGCCCCACTTCTTCA-3′	5′-AGTAGAGGGCATTCACCAGCACCA-3′	30
PAI-2	5′-CTCAAACCAAAGGTGAAATCCCAA-3′	5′-GGTATGCTCTCATGCGAGTTCACA-3′	30
Maspin	5′-CACAGATGGCCACTTTGAGGACAT-3′	5′-GGGAGCACAATGAGCATACTCAGA-3′	27
Protease nexin-1	5′-GGTCCTACCCAAGTTCACAGCTGT-3′	5′-AGGATTGCAGTTGTTGCTGCCGAA-3′	27
VEGF-A	5′-CCTGGTGGACATCTTCCAGGAGTA-3′	5′-CTCACCGCCTCGGCTTGTCACA-3′	33
FGF-1	5′-GGCTGAAGGGGAGATCACAACCTT-3′	5′-CATTTGGTGTCTGCGAGCCGTATA-3′	29
Mucin-1	5′-GTGCTGGTCTGTATTTTGGTTGCT-3′	5′-GTCACCACAGCTGGGTTGGTATAA-3′	27
Ncam-1	5′-GCTATCTGGAGGTGACCCCAGATT-3′	5′-CCTCCATGTTGGCTTCTTTGGCAT-3′	27
28s	5′-GTTCACCCACTAATAGGGAACGTGA-3′	5′-GATTCTGACTTAGAGGCGTTCAGT-3′	15

TIMP, tissue inhibitor of metalloprotease; VEGF, Vascular endothelial growth factor.

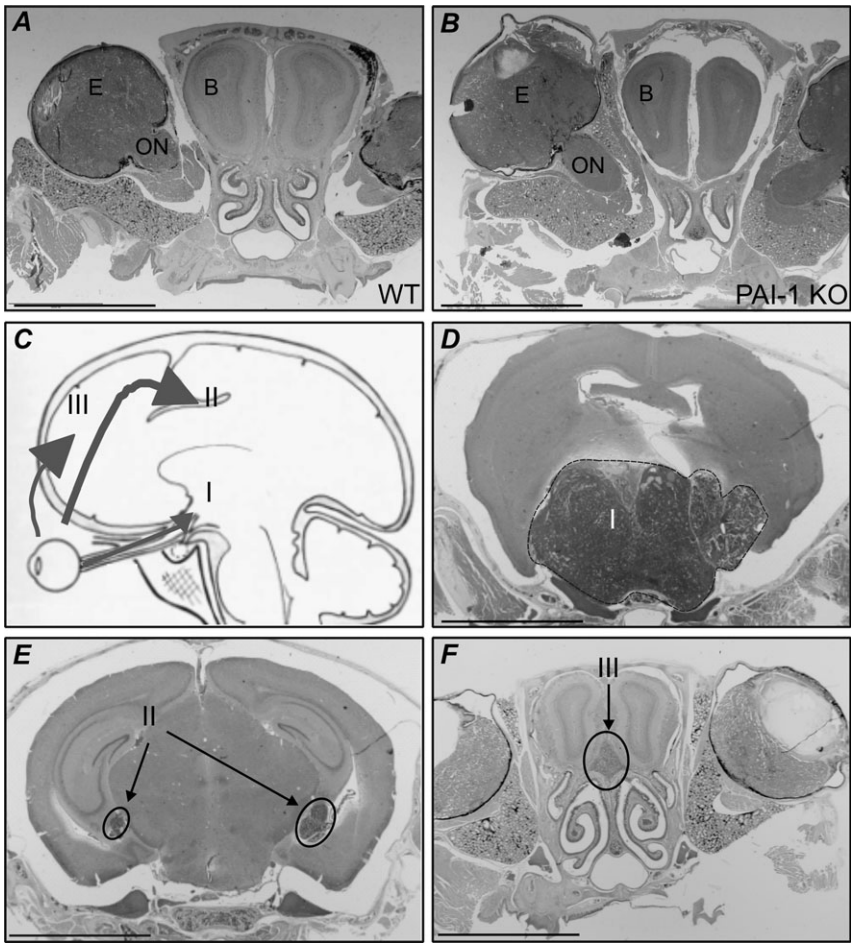

Fig. 1. (**A** and **B**) Frontal sections (5 μm) of the head crossing the middle of the eyes, from *TRP-1* WT (**A**) and *TRP-1 PAI-1* KO (PAI-$1^{-/-}$) mice (**B**). Mice were killed 64 days after birth and histological sections were stained with hematoxylin and eosin (**C**–**F**). Localization of metastasis in the brain. (**C**) Schematic sagittal section of the head visualizing the three preferential sites of metastases (I, II and III). (**D**–**F**) Frontal brain sections stained with hematoxylin and eosin. Tumor cells invading optic nerves formed nodules in the brain parenchyma adjacent to these nerves (I in panels C and D). Some metastases disseminated in the meningeal spaces (II in panels C and E). Nodules were also detected between the two olfactory lobes in frontal sections crossing the eyes (III in panels C and F). E, primary eye tumor; ON, optic nerve; B, brain. Original magnification ×10. Bars, 2 mm.

in human carcinomas of the RPE (25). These tumors are poorly infiltrated by stromal strand with rare fibroblast infiltration as assessed by S100A4 protein/fibroblast-specific protein-1 and α smooth muscle actin immunostainings (data not shown). No difference in tumor histology or vascularization was observed between the two experimental groups (data not shown).

The development of brain metastases is delayed in PAI-1 knockout mice

Brain metastases developed in 100% of 2-month-old *TRP-1* transgenic mice. They were quantified by cutting the head of each mouse ($n = 22$ for *PAI-1*$^{-/-}$ and $n = 19$ for WT mice) frontally into five distinct fragments. Sections (5 μm) were prepared from each fragment and metastasis nodules were counted on each slide (five per animal). Since brain metastases occurred preferentially at three sites, the distribution of metastases (disseminated foci versus local foci expanding from optic nerve invasion) was also analyzed (Figure 1C–F).

For all secondary nodules detected in the brain, both the incidence (percentage of animals with metastases) and severity (number of metastatic nodules per animal) of metastases were affected by *PAI-1* deficiency. *PAI-1*-deficient mice had fewer secondary lesions than corresponding WT mice. The mean number of metastases per animal was 2.5 ± 0.3 nodules in *PAI-1*$^{-/-}$ versus 3.7 ± 0.5 nodules in WT mice ($P = 0.02$) (Figure 2A). In the absence of *PAI-1*, 14% of mice did not display metastasis (severity 0), whereas 100% of WT animals showed brain metastases. Severity 2 (more than five nodules per mouse) metastasis was observed in 37% of WT animals, but in none of the *PAI-1*$^{-/-}$ transgenic mice ($P < 0.01$).

The main localization of secondary foci was brain parenchyma basis where optic nerves infiltrated by tumor cells come into close contact with brain parenchyma (I in Figure 1C and D). These nodules correspond to local invasion through optic nerve infiltration rather than to distant metastases. Metastatic nodules were found in scissura or meningeal spaces (II in Figure 1C and E) and in the anterior part of the brain, between the two olfactory lobes (III in Figure 1C and F). These three topographic distributions were frequently found in control mice. In sharp contrast, most of the secondary foci in *PAI-1*-deficient animals expanded from the brain base through optic nerve infiltration, with other distant nodules found only rarely. Indeed, WT mice developed significantly more disseminated brain nodules than did *PAI-1* knockout (KO) animals (1.7 ± 0.3 nodules in WT versus 1 ± 0.2 nodules in *PAI-1*$^{-/-}$ mice, $P = 0.03$) (Figure 2B and C).

Metastatic brain invasion led to animal death. Transgenic *PAI-1*$^{-/-}$ mice had fewer brain metastases, but survival was not affected by PAI-1 status ($n = 16$). The median survival was 95 days for *PAI-1*$^{-/-}$ mice and 92.5 days for WT mice (data not shown).

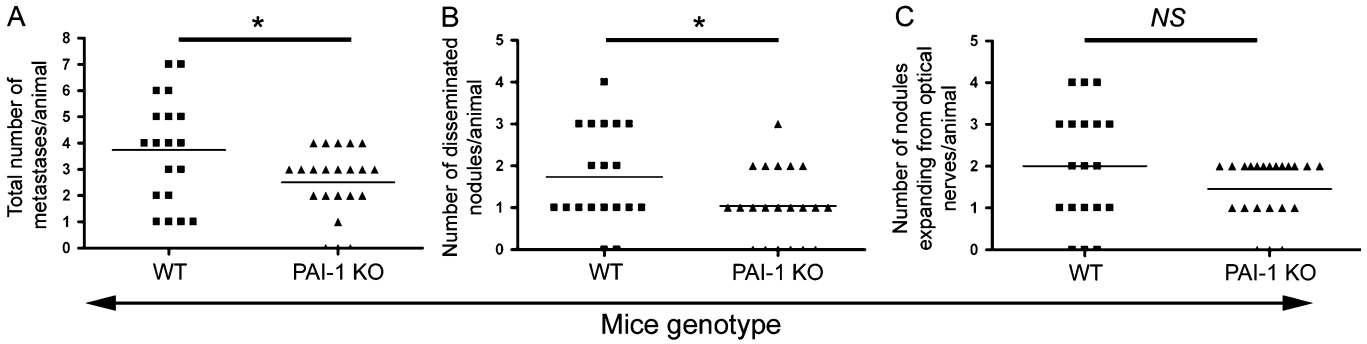

Fig. 2. Quantification of brain metastases in *TRP-1 PAI-1*$^{-/-}$ and *TRP-1* control animals. *TRP-1 PAI-1*$^{+/+}$ (WT, filled squares, $n = 19$) and *TRP-1 PAI-1*$^{-/-}$ (filled triangles, $n = 22$) mice were killed 64 days after birth. For each animal, nodules were counted on five different brain sections stained with hematoxylin and eosin to obtain a total number of metastases per animal (**A**). Disseminated nodules were quantified by counting the total number of nodules in the anterior part of the brain (between the two olfactory lobes) and in meningeal spaces (**B**) (see the legend to Figure 1). Nodules expanding from optic nerves correspond to the infiltration of one or two optic nerves and propagation to close cerebral parenchyma (**C**). Horizontal bars represent median values; *P*-values correspond to the Mann–Whitney test ($^*P \leq 0.05$; NS, non-significant value).

Motility of RPE tumor cells in vitro

In order to determine whether *PAI-1* deficiency could modulate tumor cell motility, RPE tumor cells were isolated from *TRP-1/SV40* mice proficient ($n = 5$) or deficient ($n = 5$) in *PAI-1*. Five independent cultures were established from eye tumors issued from PAI-1$^{-/-}$ and PAI-1$^{+/+}$ mice. The expression of SV40 T antigen was analyzed by immunostaining to characterize these cells. One hundred percent of cells were RPE and cultures were not contaminated by other cell types (data not shown). *PAI-1*$^{+/+}$ and *PAI-1*$^{-/-}$ cells exhibited similar migratory properties as assessed in Boyden chamber assay (Figure 3).

Expression patterns of several factors during tumor follow-up

As *PAI-1* deficiency delayed the development of brain metastasis but did not influence primary tumor progression in the *TRP-1/SV40 Tag* line, we hypothesized that other components of related proteolytic systems might compensate for the absence of PAI-1. The expression of genes encoding several protease-related candidates was evaluated by semiquantitative RT–PCR analysis on primary ocular tumors. The molecules studied included components of the plasminogen/plasmin system (tPA, uPA, uPAR, PAI-1, PAI-2, protease nexin-1 and Maspin), several members of metalloproteinase family putatively involved in angiogenesis [matrix metalloproteinase (MMP)-2, MMP-9, MMP-13 and MMP-14] and their inhibitors [tissue inhibitor of metalloprotease (TIMP)-1, TIMP-2, TIMP-3 and RECK] and the most important known angiogenic factor, vascular endothelial growth factor (VEGF)-A. PAI-1 expression levels were used as an internal control. All the factors studied displayed similar levels of expression in presence and absence of PAI-1, with the exception of TIMP-2 for which larger amounts of mRNA were produced in *PAI-1*$^{-/-}$ mice than in WT mice (0.92 ± 0.05 arbitrary units in KO mice versus 0.76 ± 0.02 in WT mice, $P = 0.005$) (Table II).

We extended this expression profiling, using a GEarray containing 96 complementary DNA fragments printed in quadruplicate (tetraspots) on a nylon membrane. We identified four genes upregulated by a factor of 1.8–2.2 in KO mice: FGF-1, Mucin-1, Ncam-1 and TIMP-2 (Table II). Array verification by semiquantitative RT–PCR on samples identical to those used for array analysis confirmed the upregulation of FGF-1 ($P = 0.001$) (Figure 4A) and TIMP-2 ($P = 0.05$) mRNA levels in *PAI-1*-deficient animals, but not that of Ncam-1 and Mucin-1 levels (data not shown).

TIMP-2 protein levels were shown, by enzyme-linked immunosorbent assay, to be similar in *TRP-1 PAI-1*-deficient and -proficient mice ($P = 0.7$, data not shown). In contrast, levels of FGF-1 production, assessed by western blotting, were higher in ocular tumors of *TRP-1 PAI-1*$^{-/-}$ mice than in those of their controls ($P = 0.008$, Figure 4B).

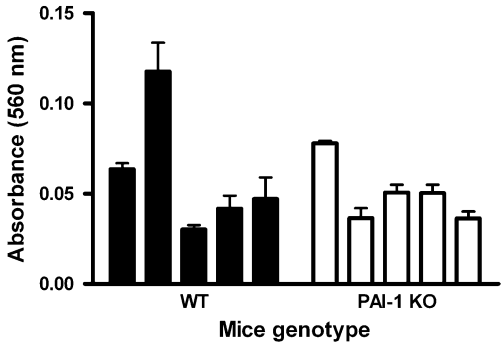

Fig. 3. *In vitro* chemotactic test of five primary RPE tumor cultures established from *TRP-1 PAI-1* WT (WT 1–5, black bars) and *PAI-1*$^{-/-}$ (KO 1–5, white bars) mice. Migrating cells were quantified by colorimetric measurement with crystal violet after 5 h of incubation time. Results (from triplicate samples) are those of one representative experiment among three separate assays. Data are presented as mean ± SE of the mean; *P*-values (P=1) correspond to the Mann–Whitney test.

Discussion

Recent studies identified PAI-1 as being causally involved in tumor progression, pointing to PAI-1 as a potential therapeutical target (1,2,9,26). However, conflicting results have been obtained, possibly due to the great diversity of experimental models used (tumor type, number of tumor cells and implantation site), the multiple functions of PAI-1 and its dose-dependent effects. In addition, further studies in spontaneous carcinogenesis models are required. To determine whether other Serpins or angiogenic factors could substitute for PAI-1 (2), we investigated the contribution of PAI-1 to spontaneous metastasis, using a model of ocular carcinogenesis including all stages of cancer progression and metastasis formation. By crossing a *PAI-1*-null allele into *TRP-1* mice, we provide the first evidence that while PAI-1 promotes distant metastases in a transgenic tumor model, increases in the production of an angiogenic factor, FGF-1, might account for similar primary tumor growth in *PAI-1*-deficient and -proficient mice.

Primary tumor growth and vascularization were found to be similar in *PAI-1*-proficient and -deficient mice. However, this does not exclude the possibility that PAI-1 contributes to earlier steps in cancer progression. We previously showed, in murine and human skin carcinomas (15,17,27), that PAI-1 is a proangiogenic factor and a crucial determinant of tumor microenvironment regulating early stages of primary tumor implantation and growth. However, once the tumor has developed, PAI-1 is no longer essential for cancer progression

(17). Accordingly, *PAI-1* deficiency does not affect primary tumor development in MMTV-PymT model (24). The similar development of primary tumors in both genotypes allowed unbiased comparison of metastases. We show here that *PAI-1* deficiency is associated with smaller numbers of brain metastases. We also found that the distribution of metastases was different in *PAI-1*$^{+/+}$ and *PAI-1*$^{-/-}$ brains. Secondary foci in *PAI-1*$^{-/-}$ mice were mostly derived from local infiltration of optic nerves, expanding toward brain parenchyma, whereas more distant metastatic foci were detected in the scissura and meningeal spaces of WT animals. This difference in the number and localization of brain metastases could not be explained by a reduction of RPE cell motility in *PAI-1*-deficient mice. Indeed, similar migratory properties were evidenced when tumor cell cultures were established from *PAI-1*-deficient or -proficient eye tumors.

Table II. Studies of gene expression by semiquantitative RT–PCR analysis and Superarray membrane on total RNA extracted from eye tumors of *TRP-1 PAI-1*$^{-/-}$ (KO) and TRP-1 *PAI-1*$^{+/+}$ (WT) mice

	Semiquantitative RT–PCR	GEarray
Plasminogen/plasmin system		
uPA	=	=
tPA	=	=
uPAR	=	=
PAI-1	WT > KO	WT > KO
PAI-2	=	=
PN-1	=	Absent from the membrane
Maspin	=	=
MMPs and their inhibitors		
MMP-2	=	=
MMP-9	=	=
MMP-14	=	=
MMP-13	=	=
TIMP-1	=	=
TIMP-2	KO > WT	KO > WT
TIMP-3	=	=
RECK	=	Absent from the membrane
Angiogenic factor: VEGF-A	=	=
Other regulated factors		
FGF-1		KO > WT
Mucin-1		KO > WT
Ncam-1		KO > WT

=, Similar expression level; WT > KO, higher expression level in WT than in KO mice; KO > WT, higher expression level in KO than in WT mice.
TIMP, tissue inhibitor of metalloprotease; VEGF, vascular endothelial growth factor.

A possible explanation for the lack of effect of *PAI-1* deficiency on the growth of primary *TRP-1/SV40 Tag* eye tumors is a functional overlap between PAI-1 and other protease inhibitors. We therefore searched for functional redundancy, focusing on alternative inhibitors of matrix remodeling (PAI-2, protease nexin-1, Maspin, TIMPs) and other compounds of PA and MMP proteolytic systems putatively involved in angiogenesis. Such a functional overlap between MMP and PA systems has been demonstrated in wound healing (28). However, our transgenic tumor model provided no evidence that *PAI-1* deficiency led to functional redundancy or a compensatory increase in the levels of proteases or their inhibitors. By using a more global approach based on Superarray GEarray technology, increased FGF-1 production in primary tumors was detected at mRNA levels and confirmed at protein levels. FGF-1 is not only angiogenic but also acts as an important survival factor for normal RPE cells or endothelial cells (29–32). FGF-1 probably promotes primary RPE tumor growth and angiogenesis through several mechanisms.

There is an apparent discrepancy between the dramatic effects of *PAI-1* deficiency in transplanted human and murine tumor models (15–17,26) and the absence of an impact on spontaneous tumor development in carcinogenesis models, such as *MMTV-PymT* (24) and *TRP-1/SV40 Tag* transgenic mice. One possible reason is that compensatory mechanisms, such as angiogenic molecule production, can take place in transgenic mice during development and growth, but not in mice challenged by massive tumor cell injections. FGF-1 is specifically upregulated during tumor growth since no FGF-1 increase was evidenced in eyes and brains of non-tumor-bearing *PAI-1*-deficient mice (data not shown). Therefore, the FGF-1 upregulation observed in the absence of PAI-1 is not an inherent response during animal development, but it is associated to the tumorigenic process.

The higher levels of FGF-1 production observed in *TRP-1/SV40 Tag* tumors were not detected in the skin transplantation model used in

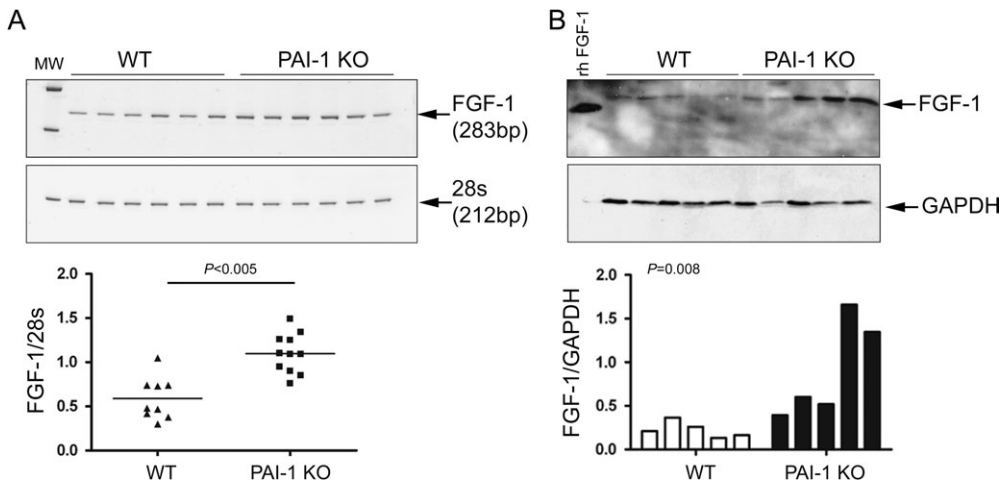

Fig. 4. Analysis of FGF-1 expression at the mRNA (**A**) and protein (**B**) levels. (**A**) Gene array verification by semiquantitative RT–PCR analysis of FGF-1 expression. Total RNA was extracted from eye tumors of 11 *TRP-1 PAI-1*-deficient and 9 *TRP-1* control mice killed on day 64. For FGF-1 PCR products, the upper panel shows a representative polyacrylamide gel with six representative samples from WT (left part) and *PAI-1* KO mice (right part). The expected sizes of amplified products are indicated on the right. Scatter plot (below panel) corresponds to the densitometric quantification of PCR products. Results are expressed as amplified mRNA level divided by 28S ribosomal RNA level. Horizontal bars indicate mean values; *P*-values indicated correspond to Mann–Whitney tests. (**B**) Western blot analysis of FGF-1 production in *TRP-1* transgenic mice with and without deletion of *PAI-1* gene. The upper panel shows western blot analysis of five representative samples from *WT* and *PAI-1*$^{-/-}$ mice. Recombinant human (rh) FGF-1 was used as positive control. GAPDH protein levels were assessed as a loading control. Quantification of FGF-1 production by scanning densitometry in WT (white bars) and *PAI-1*$^{-/-}$ (black bars) mice (below panel). Results are expressed as FGF-1 protein levels divided by GAPDH protein levels. *P*-values indicated correspond to Mann–Whitney test.

previous studies (15) (data not shown). This suggests that FGF-1 overproduction may be specific to RPE tumors or take place throughout pathological angiogenesis, as a host response, and not during transient challenge. Carcinogenesis models thus better reflect the real pathogenesis of cancer and may provide important information regarding host reaction to the long-term inhibition or deletion of a specific gene product.

PAI-1 is a multifunctional protein. In addition to its Serpin function, it also binds to vitronectin, thereby regulating cell adhesion and migration (7). This protein also has a low-density lipoprotein receptor-related protein-binding site involved in controlling cell migration via uPA/uPAR internalization (33) and in regulating cell proliferation and apoptosis via the phosphoinositide-3 kinase–AKT pathway (8). To dissect functional properties of PAI-1, we and others have used mutated forms of recombinant PAI-1 that unraveled novel PAI-1 activities unrelated to serine protease-inhibitory activity (8,11,13,27, 34). However, this strategy is hampered in the present model by the occurrence of tumor transformation and progression *in utero* and the impossibility of using adenovirus-mediated gene transfer or recombinant protein injection at early stages. In addition, the anatomy of the eye hinders the access of pharmacological compounds to intraocular environment in neonatal or adult mice (35).

Pharmacological compounds modulating PAI-1 activities are currently under development (2,36–40). However, particular features of PAI-1 might raise concerns about its targeting for treatment purposes and should be carefully addressed: (i) its multifunctionality; (ii) its short half-life *in vivo*; (iii) its dose-dependent effect and finally (iv) its impact on the fibrinolytic system and on the process of atherosclerosis and thrombosis. A strategy based on the use of specific stabilized mutants interfering with binding to vitronectin, but without affecting PA activity, can be used to block angiogenesis without affecting fibrinolysis or thrombosis (13). Despite major progress toward the development of pharmacological PAI-1 inhibitors, there is currently no evidence to suggest that compensatory mechanisms are induced following the deletion or long-term inhibition of PAI-1. Our study provides the first evidence of an increase in FGF-1 production in the absence of *PAI-1* gene. This may account for the lack of a phenotype in the development of primary tumors in *PAI-1*-deficient mice and may, at least partly, account for some of the conflicting data reported in previous studies. Our data highlight the need for further investigations before the clinical use of PAI-1-targeting compounds. The recent approval of antiangiogenic agents for clinical applications has not only provided a proof of concept for antiangiogenic strategies but has also highlighted the possible progressive emergence of resistance to treatment (41). It should be noted that FGF-1 has been reported to be upregulated and functionally involved in the regrowth of tumors that manifest such a phenotypic resistance to VEGF receptor 2 blockage in human tumors (42). Our data suggest that the long-term targeting of PAI-1 might be counteracted by the overproduction of angiogenic factors, such as FGF-1. Further studies, in other models, are urgently required to address this important issue.

Funding

European Union Framework Programme 6 projects (LSHC-CT-2003-503297 'CANCERDEGRADOME', LSHC-CT-2004-503224 BRECOSM); Framework Programme 6-NOE (LSHM-CT-2004-512040 EMBIC) FP7-HEALTH-2007-A Proposal No. 201279 'MICROENVIMET'); Fonds de la Recherche Scientifique Médicale, Fonds National de la Recherche Scientifique (Belgium), Fondation contre le Cancer, C.G.R.I.-F.N.R.S.-INSERM Coopération, Fonds spéciaux de la Recherche (University of Liège); Centre Anticancéreux près l'Université de Liège, Fonds Léon Fredericq (University of Liège); D.G.T.R.E. from the Région Wallonne (616476 NEOANGIO); Fonds Social Européen; Fonds d'Investissements de la Recherche Scientifique (CHU, Liège, Belgium); Interuniversity Attraction Poles Programme—Belgian Science Policy (Brussels, Belgium); FNRS-Télévie to C M., M.M., M.J. and A.M.

Acknowledgements

We thank E. Connault, G. Roland, P. Gavitelli, I. Dasoul, E. Feyereisen, E. Konradowski, M. R. Pignon and F. Olivier for excellent technical assistance.

Conflict of Interest Statement: None declared.

References

1. Rakic,J.M. *et al*. (2003) Role of plasminogen activator-plasmin system in tumor angiogenesis. *Cell. Mol. Life Sci.*, **60**, 463–473.
2. Andreasen,P.A. (2007) PAI-1-a potential therapeutic target in cancer. *Curr. Drug Targets*, **8**, 1030–1041.
3. Dass,K. *et al*. (2008) Evolving role of uPA/uPAR system in human cancers. *Cancer Treat. Rev.*, **34**, 122–136.
4. Potempa,J. *et al*. (1994) The serpin superfamily of proteinase inhibitors: structure, function, and regulation. *J. Biol. Chem.*, **269**, 15957–15960.
5. Stefansson,S. *et al*. (1996) The serpin PAI-1 inhibits cell migration by blocking integrin alpha V beta 3 binding to vitronectin. *Nature*, **383**, 441–443.
6. Deng,G. *et al*. (2001) Plasminogen activator inhibitor-1 regulates cell adhesion by binding to the somatomedin B domain of vitronectin. *J. Cell. Physiol.*, **189**, 23–33.
7. Czekay,R.P. *et al*. (2004) Unexpected role of plasminogen activator inhibitor 1 in cell adhesion and detachment. *Exp. Biol. Med. (Maywood)*, **229**, 1090–1096.
8. Balsara,R.D. *et al*. (2006) A novel function of plasminogen activator inhibitor-1 in modulation of the AKT pathway in wild-type and plasminogen activator inhibitor-1-deficient endothelial cells. *J. Biol. Chem.*, **281**, 22527–22536.
9. Duffy,M.J. *et al*. (2008) Cancer invasion and metastasis: changing views. *J. Pathol.*, **214**, 283–293.
10. Devy,L. *et al*. (2002) The pro- or antiangiogenic effect of plasminogen activator inhibitor 1 is dose dependent. *FASEB J.*, **16**, 147–154.
11. Lambert,V. *et al*. (2003) Dose-dependent modulation of choroidal neovascularization by plasminogen activator inhibitor type I: implications for clinical trials. *Invest. Ophthalmol. Vis. Sci.*, **44**, 2791–2797.
12. McMahon,G.A. *et al*. (2001) Plasminogen activator inhibitor-1 regulates tumor growth and angiogenesis. *J. Biol. Chem.*, **276**, 33964–33968.
13. Stefansson,S. *et al*. (2001) Inhibition of angiogenesis *in vivo* by plasminogen activator inhibitor-1. *J. Biol. Chem.*, **276**, 8135–8141.
14. Bajou,K. *et al*. (2004) Host-derived plasminogen activator inhibitor-1 (PAI-1) concentration is critical for *in vivo* tumoral angiogenesis and growth. *Oncogene*, **23**, 6986–6990.
15. Bajou,K. *et al*. (1998) Absence of host plasminogen activator inhibitor 1 prevents cancer invasion and vascularization. *Nat. Med.*, **4**, 923–928.
16. Gutierrez,L.S. *et al*. (2000) Tumor development is retarded in mice lacking the gene for urokinase-type plasminogen activator or its inhibitor, plasminogen activator inhibitor-1. *Cancer Res.*, **60**, 5839–5847.
17. Maillard,C. *et al*. (2005) Host plasminogen activator inhibitor-1 promotes human skin carcinoma progression in a stage-dependent manner. *Neoplasia*, **7**, 57–66.
18. Soff,G.A. *et al*. (1995) Expression of plasminogen activator inhibitor type 1 by human prostate carcinoma cells inhibits primary tumor growth, tumor-associated angiogenesis, and metastasis to lung and liver in an athymic mouse model. *J. Clin. Invest.*, **96**, 2593–2600.
19. Praus,M. *et al*. (1999) Reduction of tumor cell migration and metastasis by adenoviral gene transfer of plasminogen activator inhibitors. *Gene Ther.*, **6**, 227–236.
20. Ma,D. *et al*. (1997) Inhibition of metastasis of intraocular melanomas by adenovirus-mediated gene transfer of plasminogen activator inhibitor type 1 (PAI-1) in an athymic mouse model. *Blood*, **90**, 2738–2746.
21. Tsuchiya,H. *et al*. (1997) Plasminogen activator inhibitor-1 accelerates lung metastasis formation of human fibrosarcoma cells. *Anticancer Res.*, **17**, 313–316.
22. Tsuchiya,H. *et al*. (1995) The antibody to plasminogen activator inhibitor-1 suppresses pulmonary metastases of human fibrosarcoma in athymic mice. *Gen. Diagn. Pathol.*, **141**, 41–48.
23. Eitzman,D.T. *et al*. (1996) Lack of plasminogen activator inhibitor-1 effect in a transgenic mouse model of metastatic melanoma. *Blood*, **87**, 4718–4722.
24. Almholt,K. *et al*. (2003) Metastasis of transgenic breast cancer in plasminogen activator inhibitor-1 gene-deficient mice. *Oncogene*, **22**, 4389–4397.
25. Penna,D. *et al*. (1998) Tumors of the retinal pigment epithelium metastasize to inguinal lymph nodes and spleen in tyrosinase-related protein 1/SV40 T antigen transgenic mice. *Oncogene*, **17**, 2601–2607.

26. Lee,C.C. *et al*. (2005) Plasminogen activator inhibitor-1: the expression, biological functions, and effects on tumorigenesis and tumor cell adhesion and migration. *J. Cancer Mol.*, **1**, 25–36.
27. Bajou,K. *et al*. (2001) The plasminogen activator inhibitor PAI-1 controls *in vivo* tumor vascularization by interaction with proteases, not vitronectin. Implications for antiangiogenic strategies. *J. Cell Biol.*, **152**, 777–784.
28. Lund,L.R. *et al*. (1999) Functional overlap between two classes of matrix-degrading proteases in wound healing. *EMBO J.*, **18**, 4645–4656.
29. Bryckaert,M. *et al*. (2000) Regulation of proliferation-survival decisions is controlled by FGF1 secretion in retinal pigmented epithelial cells. *Oncogene*, **19**, 4917–4929.
30. Guillonneau,X. *et al*. (1997) FGF2-stimulated release of endogenous FGF1 is associated with reduced apoptosis in retinal pigmented epithelial cells. *Exp. Cell Res.*, **233**, 198–206.
31. Xue,L. *et al*. (2002) Angiogenic effect of fibroblast growth factor-1 and vascular endothelial growth factor and their synergism in a novel *in vitro* quantitative fibrin-based 3-dimensional angiogenesis system. *Surgery*, **132**, 259–267.
32. Uriel,S. *et al*. (2006) Sustained low levels of fibroblast growth factor-1 promote persistent microvascular network formation. *Am. J. Surg.*, **192**, 604–609.
33. Herz,J. *et al*. (2001) LRP: a multifunctional scavenger and signaling receptor. *J. Clin. Invest.*, **108**, 779–784.
34. Praus,M. *et al*. (2002) Both u-PA inhibition and vitronectin binding by plasminogen activator inhibitor 1 regulate HT1080 fibrosarcoma cell metastasis. *Int. J. Cancer*, **102**, 584–591.
35. Bouquet,C. *et al*. (2003) Systemic administration of a recombinant adenovirus encoding a HSA-angiostatin kringle 1-3 conjugate inhibits MDA-MB-231 tumor growth and metastasis in a transgenic model of spontaneous eye cancer. *Mol. Ther.*, **7**, 174–184.
36. De Taeye,B. *et al*. (2004) Site-directed targeting of plasminogen activator inhibitor-1 as an example for a novel approach in rational drug design. *J. Biol. Chem.*, **279**, 20447–20450.
37. Leik,C.E. *et al*. (2006) Effect of pharmacologic plasminogen activator inhibitor-1 inhibition on cell motility and tumor angiogenesis. *J. Thromb. Haemost.*, **4**, 2710–2715.
38. Crandall,D.L. *et al*. (2004) Characterization and comparative evaluation of a structurally unique PAI-1 inhibitor exhibiting oral *in-vivo* efficacy. *J. Thromb. Haemost.*, **2**, 1422–1428.
39. Liang,A. *et al*. (2005) Characterization of a small molecule PAI-1 inhibitor, ZK4044. *Thromb. Res.*, **115**, 341–350.
40. Gils,A. *et al*. (2004) The structural basis for the pathophysiological relevance of PAI-I in cardiovascular diseases and the development of potential PAI-I inhibitors. *Thromb. Haemost.*, **91**, 425–437.
41. Carmeliet,P. (2005) Angiogenesis in life, disease and medicine. *Nature*, **438**, 932–936.
42. Casanovas,O. *et al*. (2005) Drug resistance by evasion of antiangiogenic targeting of VEGF signaling in late-stage pancreatic islet tumors. *Cancer Cell*, **8**, 299–309.

Received April 28, 2008; revised August 21, 2008; accepted August 22, 2008